Modeling of Hydrodesulfurization (HDS), Hydrodenitrogenation (HDN), and the Hydrogenation of Aromatics (HDA) in a Vacuum Gas Oil Hydrotreater

M. A. Rodríguez[†,‡] and J. Ancheyta*[,†]

Instituto Mexicano del Petróleo, Eje Central Lázaro Cárdenas 152, Col. San Bartolo Atepehuacan, México D.F. 07730 Mexico, and Facultad de Ingeniería, UNAM, Ciudad Universitaria, México D.F. 04510

Received October 23, 2003

A trickle-bed reactor model has been used in this work to simulate the catalytic hydrotreating of oil fractions. The most important reactions (hydrodesulfurization (HDS), hydrodenitrogenation (HDN), and the hydrogenation of aromatics (HDA)) are taken into account in the model. Kinetics of each reaction and reactor model was taken from different sources in the literature. HDS reaction was described by Langmuir−Hinshelwood kinetics. HDN was modeled as a consecutive reaction scheme in which nonbasic compounds are hydrogenated first to basic nitrogen compounds, which undergo further reactions to eliminate the N atom from the molecule. The kinetics of aromatics hydrogenation was represented by a first-order reversible reaction. The reactor model includes correlations for determining mass-transfer coefficients and is based on the two-film theory. The model was tested with experimental information obtained at pilot scale during the hydrotreating of vacuum gas oil. The pilot reactor was operated under isothermal conditions, and the effect of reaction temperature and space velocity on HDS, HDN, and HDA was studied in the ranges of 360−380 °C and 2 h^{-1}, respectively. The predicted results showed good agreement with the experimental information. The model was also applied for simulating the behavior of a NiMo catalyst during commercial nonisothermal operation of an industrial hydrotreating plant.

Introduction

Catalytic hydrotreating (HDT) is one of the most important processes in the petroleum refining industry. The HDT process is applied to treat a great variety of refinery streams, such as straight-run distillates, vacuum gas oils (fluidized catalytic cracking (FCC) feed), atmospheric and vacuum residua, light cycle oil, FCC naphtha, lube oils, etc. The main differences for the hydrotreating processes of each feed are operating conditions (temperature, H_2 partial pressure, H_2-to-oil ratio, space velocity), type of catalyst (NiMo, CoMo, etc.), reactor configuration (single reactor, reactors in series, one catalytic bed with various catalysts), and reaction system (fixed bed, ebullated bed, slurry).

Depending on the feed and the main objective of the treatment, the process can be called hydrodesulfurization (HDS), as in the case of the naphtha, which is used as reforming feed where sulfur is the main undesirable heteroatom. For straight-run gas oil, the process is called hydrotreating because, in addition to sulfur, aromatic saturation and nitrogen removal are also desired for diesel fuel production.[1] A hydrodemetallization process is used for the removal of vanadium and nickel from heavy oils. When a change in the molecular weight of the feed is required, a hydrocracking process is used.[2]

For light feeds, the reactions are frequently performed in two-phase (gas−solid) fixed-bed reactors. However, when the instillation range of the feed increases, three phases are commonly found: hydrogen, a liquid−gas mixture of the partially vaporized feed, and the solid catalyst.[3] This latter system is called a trickle-bed reactor (TBR), which is referenced in the literature as a reactor in which a liquid phase and a gas phase flow concurrently downward through a fixed-bed of catalyst particles while reactions occur.[4]

TBR reactors have been the subject of many investigations, and various authors have summarized them in different reviews. The most-recent recompilation and analysis of these reactors were presented by Dudokovic et al.[5] This type of reactor has also received attention from the modeling point of view. Different approaches have been utilized with different level of sophistication. Some authors have used pseudo-homogeneous models without distinction between the liquid/gas phase and the solid catalyst, and others have taken into account mass transfer between the phases.[6−8]

In addition to the sophistication of the reactor model, reaction kinetics is also another important difference.

* Author to whom correspondence should be addressed. E-mail address: jancheyt@imp.mx.
† Instituto Mexicano del Petroleo.
‡ UNAM, Ciudad Universitaria.

(1) Marroquín, G.; Ancheyta, J. *Appl. Catal., A* **2001**, *207*, 407−420.
(2) Ancheyta, J.; Betancourt, G.; Marroquín, G.; Pérez, A.; Maity, S. K.; Cortes, M. T.; del Río, R. *Energy Fuels* **2001**, *15*, 120−127.
(3) Ancheyta, J.; Marroquín, G.; Angeles, M. J.; Macías, M. J.; Pitault, I.; Forissier, M.; Morales, R. D. *Energy Fuels* **2002**, *16*, 1059−1067.
(4) Satterfield, C. N. *AIChE J.* **1975**, *21*, 209.
(5) Dudukovic, M. P.; Larachi, F.; Mills, P. L. *Catal. Rev.* **2002**, *44*, 123−246.
(6) Korsten, H.; Hoffmann, U. *AIChE J.* **1996**, *42*, 1350−1360.

10.1021/ef030172s CCC: $27.50
Published on Web 04/16/2004

Table 1. Correlations Used in the Model of Korsten and Hoffmann[a]

parameter	correlation
oil density	$\rho(p,T) = \rho_0 + \Delta\rho_p - \Delta\rho_T$
	$\Delta\rho_p = [0.167 + (16.181 \times 10^{-0.0425\rho_0})]\left(\frac{p}{1000}\right) - 0.01[0.299 + (263 \times 10^{-0.0603\rho_0})]\left(\frac{p}{1000}\right)^2$
	$\Delta\rho_T = [0.0133 + 152.4(\rho_0 + \Delta\rho_p)^{-2.45}](T - 520) - [8.1 \times 10^{-6} - 0.0622 \times 10^{-0.764(\rho_0+\Delta\rho_p)}](T - 520)^2$
Henry coefficient	$H_i = \frac{v_N}{\lambda_i \rho_L}$
solubility of hydrogen	$\lambda_{H_2} = -0.559729 - 0.42947 \times 10^{-3}T + 3.07539 \times 10^{-3}\left(\frac{T}{\rho_{20}}\right) + 1.94593 \times 10^{-6}T^2 + \frac{0.835783}{\rho_{20}^2}$
solubility of H_2S	$\lambda_{H_2S} = \exp(3.3670 - 0.008470T)$
gas−liquid mass-transfer coefficient	$\frac{k_i^L a_L}{D_i^L} = 7\left(\frac{G_L}{\mu_L}\right)^{0.4}\left(\frac{\mu_L}{\rho_L D_i^L}\right)^{1/2}$
dynamic liquid viscosity	$\mu_L = 3.141 \times 10^{10}(T - 460)^{-3.444}[\log_{10}(\mathrm{API})]^a$
	$a = 10.313[\log_{10}(T - 460)] - 36.447$
diffusivity	$D_i^L = 8.93 \times 10^{-8}\left(\frac{v_L^{0.267}}{v_i^{0.433}}\right)\left(\frac{T}{\mu_L}\right)$
molar volume	$v = 0.285 v_c^{1.048}$
	$v_c^m = 7.5214 \times 10^{-3}(T_{\mathrm{MeABP}}^{0.2896})(d_{15.6}^{-0.7666})$
liquid−solid mass-transfer coefficient	$\frac{k_i^S}{D_i^L a_S} = 1.8\left(\frac{G_L}{a_S \mu_L}\right)^{1/2}\left(\frac{\mu_L}{\rho_L D_i^L}\right)^{1/3}$
specific surface area	$a_S = \frac{6}{d_p}(1 - \epsilon)$

[a] From ref 6.

Most of the models only take into consideration the HDS reaction, which is also the most studied reaction and involves one of the highest pollutants to the environmental compounds. The common approaches are based on power-law or Langmuir−Hinshelwood kinetic models. However, models that involve other reactions, such as the hydrogenation of aromatics (HDA) and hydrodenitrogenation (HDN), are scarce in the literature. These other reactions are also very important for HDT reactor modeling, because, as in the case of diesel, apart from sulfur specification, environmental authorities are considering maximum limits in aromatics and nitrogen. In the case of HDT of a FCC feed, these reactions are also important, because these compounds adversely affect the behavior of the catalytic cracking units.

On the other hand, experiments for catalyst screening and process studies are mostly conducted in microreactors and pilot-plant scales. These systems commonly operate under the same conditions reported in commercial units but keep the reaction temperature constant. Because commercial HDT reactors do not operate isothermally, experimental information generated from small reactors does not represent the commercial operation exactly. One way to predict this commercial behavior from small-system results is via the use of reactor modeling.

The objective of the present work is to illustrate the use of a TBR reactor model to predict the behavior of a catalyst in a commercial HDT unit based on data obtained at pilot-plant scale.

Kinetic and Reactor Modeling

Base Model. A three-phase reactor model reported in the literature[6] was used in the present investigation. The model includes correlations for determining the mass-transfer coefficients, solubility data, and properties of oils and gases under the process conditions, using information reported in the literature,[9−14] which is summarized in Table 1.

In the literature reactor model,[6] the HDT reactor is assumed to operate at constant temperature and the kinetics for HDS reaction is described by the following Langmuir−Hinshelwood model:

$$r_{\mathrm{HDS}} = k_{\mathrm{HDS}} \frac{(C_S^S)(C_{H_2}^S)^{0.45}}{(1 + K_{H_2}^S C_{H_2S}^S)^2} \quad (1)$$

The reactor model considers that no reactions occur in the gas phase and the mass-balance equations for the gaseous components is

$$\frac{u_G}{RT}\frac{dp_i^G}{dz} + k_i^G a_L\left(\frac{p_i^G}{H_i} - C_i^L\right) = 0 \quad (2)$$

and for the gaseous compounds in the liquid phase is

$$u_L\frac{dC_i^L}{dz} - k_i^L a_L\left(\frac{p_i^G}{H_i} - C_i^L\right) + k_i^S a_S(C_i^L - C_i^S) = 0 \quad (3)$$

The mass-balance equation for the organic sulfur compounds

(7) Avraam, D. G.; Vasalos, I. A. *Catal. Today* **2003**, *79−80*, 275−283.
(8) Pedernera, E.; Reimert, R.; Nguyen, N. L.; van Buren, V. *Catal. Today* **2003**, *79−80*, 371−381.
(9) Ahmed, T. *Hydrocarbon Phase Behavior*; Gulf Publishing: Houston, TX, 1989.
(10) Goto, S.; Smith, J. M. *AIChE J.* **1975**, *21*, 706.
(11) Reid, R. C.; Prausnitz, J. M.; Poling, B. E. *The Properties of Gases and Liquids*, 4th ed.; McGraw-Hill: New York, 1987.
(12) *API Technical Data Book: Petroleum Refining*; American Petroleum Institute: Washington, DC, 1984.

and the liquid hydrocarbon is

$$u_L \frac{dC_i^L}{dz} + k_i^S a_S (C_i^L - C_i^S) = 0 \quad (4)$$

Equations 2 and 3 are developed only for hydrogen and H_2S, whereas eq 4 has been developed for organic sulfur and hydrocarbons.

The components transported between the liquid phase and the surface of the catalyst are consumed or produced by chemical reaction, according to the following equation, which is applied for hydrogen, H_2S, organic sulfur, and hydrocarbons:

$$k_i^S a_S (C_i^L - C_i^S) = -\rho_B r_i \quad (5)$$

Extended Model. As mentioned in the Introduction, apart from HDS, there are other reactions that are also important during HDT. For this reason, we have included in the above-described model the HDA and HDN reactions. The kinetics of HDA was represented by a first-order reversible reaction, and HDN was modeled as a consecutive reaction scheme in which nonbasic nitrogen (N_{NB}) compounds are hydrogenated first to basic nitrogen (N_B) compounds, which undergo further reactions to eliminate the N atom from the molecule. The following kinetic expressions of these two reactions were used:

$$r_{HDN_B} = k_{N_{NB}} (C_{N_{NB}})^{1.5} - K_{N_N} (C_{N_N})^{1.5}$$

(for basic nitrogen, from Bej et al.[15]) (6)

$$r_{HDN_{NB}} = k_{N_{NB}} (C_{N_{NB}})^{1.5}$$

(for nonbasic nitrogen, from Bej et al.[15]) (7)

$$r_{HDA} = k_f p_{H_2} C_A - k_r (1 - C_A)$$

(for the HDA, from Yui and Sanford[16]) (8)

With the inclusion of these other reactions, in addition to HDS (eq 1), eqs 2 and 3 were also developed for ammonia, eq 4 for basic and nonbasic nitrogen and aromatics compounds, and eq 5 for all components.

On the other hand, it is well-known that, because of the exothermic nature of HDT reactions, the temperature along the reactor is increased. Thus, we must be able to predict this temperature change. For this reason, we have used the following energy-balance equation:[17]

$$\frac{dT}{dz} = \sum [(-\Delta H_R)(r_i)] \frac{\epsilon_L}{u_G \rho_G c_{pG} \epsilon_G + u_L \rho_L c_{pL} \epsilon_L} \quad (9)$$

Results and Discussion

Modeling of HDT Pilot-Plant Data. Because kinetic information was taken from different sources, in which the operating conditions, the type of catalyst and feed, and the experimental setup, among other factors, are also different, it is almost impossible to have an exact representation of experimental data generated in other reaction systems, and recalculation of kinetic parameter values is mandatory.

Table 2. Kinetic Parameters of eq 1 and eqs 6−8

reaction	E_A (kJ/mol)	k_o
HDS	131.99	4.266×10^9 cm^3 g^{-1} s^{-1} cm^3 mol$^{-0.45}$
HDN_{NB}	164.94	3.62×10^6 h^{-1} wt %$^{-0.5}$
HDN_B	204.34	3.66×10^{11} h^{-1} wt %$^{-0.5}$
HDA		
forward	121.40	1.041×10^5 h^{-1} MPa^{-1}
reverse	186.40	8.805×10^9 h^{-1}

For this reason, in the present study, we have conducted some experiments in the pilot reactor using vacuum gas oil as the hydrotreating feed. The experimental work was conducted in a pilot plant that has been described in detail elsewhere.[1] A typical feed for the FCC unit (vacuum gas oil) was used for HDT tests (22°API, 2 wt % sulfur, 1284 wppm total nitrogen, 518 wppm basic nitrogen, 41.9 wt % total aromatics).

A NiMo commercial catalyst was used in all experiments. It had the following characteristics: specific surface area, 175 m^2/g; pore volume, 0.56 cm^3/g; mean pore diameter, 127 Å; Mo content, 10.7 wt %; and Ni content, 2.9 wt %.

When the catalyst was loaded into the reactor, it was diluted with an equal volume of inert material (SiC, with an average particle size of 1.4 mm), to maintain a ratio of the volume of catalyst to that of diluent at a constant value of 1.0. This inert material was used to minimize the problems when testing catalysts that have a commercially applied size and shape. Therefore, the hydrodynamics of the flowing fluids will be mainly dictated by the packing of small inert particles, whereas the catalytic conversion behavior is that of the catalyst in the actual size.

HDT pilot-plant tests were conducted under the following operating conditions: pressure, 54 kg/cm^2; hydrogen-to-oil ratio, 2000 ft^3/bbl; and liquid hourly space velocity (LHSV), 2 h^{-1}. Reaction temperature was varied in the range of 340−380 °C. The reactor temperature was maintained at the desired level using a three-zone electric furnace, which provided an isothermal temperature along the active reactor section. The greatest deviation from the desired temperature values was ∼4−5 °C. All the experiments were performed without hydrogen recycling. The purity of the hydrogen was 99.9%.

Using the experimental information about properties of the hydrotreated products (sulfur, total nitrogen, basic nitrogen, and aromatic contents), the kinetic parameters involved in eq 1 and in eqs 6−8 were estimated, which are shown in Table 2. The reason for these new parameter values is to account for all the differences previously mentioned in the experiments reported in the literature and to improve the prediction of our pilot-plant information.

The values of the kinetic parameters were calculated as a function of reaction temperature by optimizing an objective function based on the sum of square errors between experimental and calculated contaminant contents. The objective function was solved using the least-squares criterion with a nonlinear regression procedure based on Marquardt's algorithm.[18]

After the kinetic parameters were determined, simulations that used only mass-balance equations were

(13) Perry, R. H.; Green, D. *Perry's Chemical Engineers' Handbook*, 6th ed.; McGraw-Hill: New York, 1987.
(14) Froment, G. F.; Depauw, G. A.; Vanrysselberghe, V. *Ind. Eng. Chem. Res.* **1994**, *33*, 2975−2988.
(15) Bej, S. K.; Dalai, A. K. Adjaye, J. *Energy Fuels* **2001**, *15*, 377−383.
(16) Yui, S. M.; Sanford, E. C. *1985 Proceedings—Refining Department: 50th Midyear Meeting* (Kansas City, MO, May 13-16, 1985); American Petroleum Institute: Washington, DC, 1985; pp 290−297.
(17) Tarhan, O. M. *Catalytic Reactor Design*; McGraw-Hill: New York, 1983.
(18) Marquardt, D. W. *J. Soc. Ind. Appl. Math.* **1963**, *2*, 431−441.

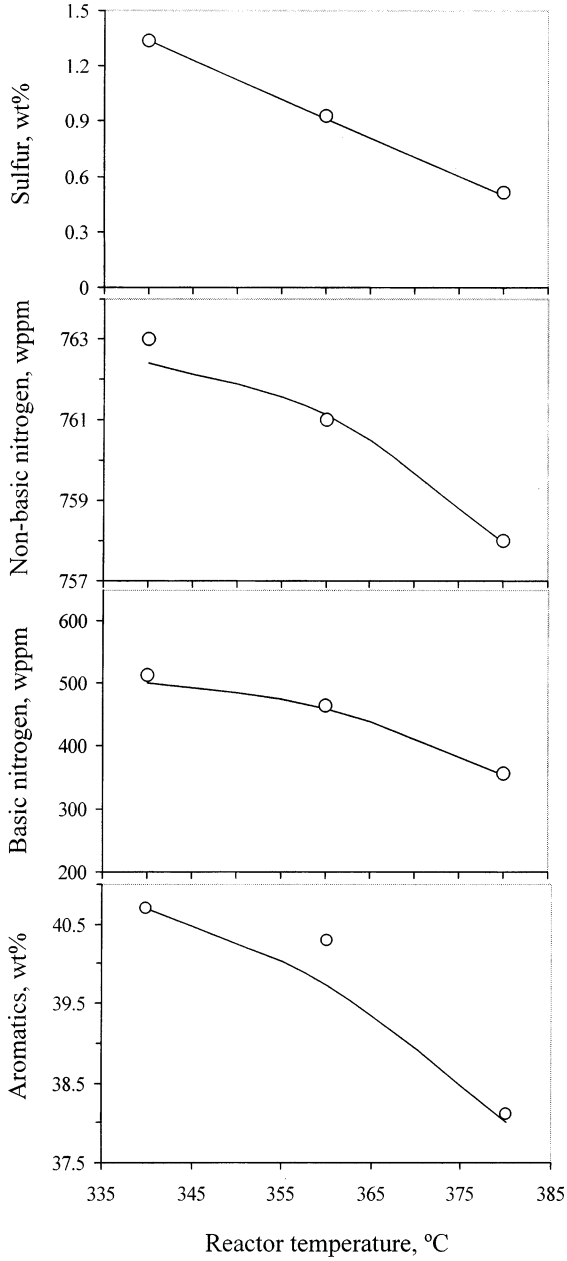

Figure 1. Comparison between experimental (symbols, ○) and predicted (line/curve) contaminant contents in the product.

performed, because the pilot reactor operates at constant temperature. Figure 1 shows a comparison between experimental and calculated mass concentrations of sulfur, basic nitrogen, total nitrogen, and aromatics, as a function of reaction temperature. The model is observed to accurately predict experimental data obtained at isothermal reactor mode of operation. The average absolute error for all predictions is <2%.

The simulated molar concentration profiles in the reactor, based on the parameters given earlier, are shown in Figures 2 and 3. It is observed that the concentrations of sulfur, nitrogen, and aromatics (Figure 2), and that of hydrogen and H_2S (Figure 3), in both the liquid and solid phases are not equal along the reactor.

The gradients of concentrations are more or less constant along the reactor. Hydrogen and H_2S exhibit the highest difference in concentration gradients in the solid and liquid phases. The balance between reaction

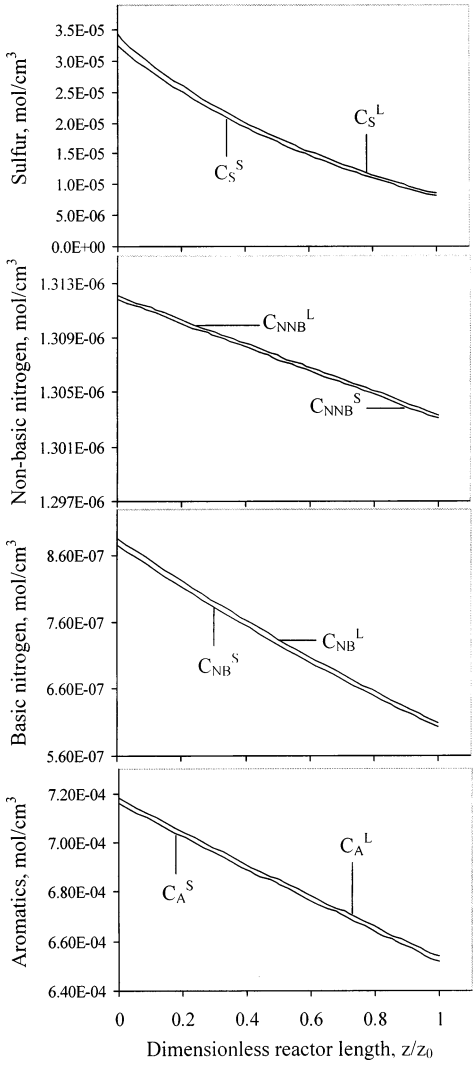

Figure 2. Concentrations of sulfur, nitrogen, and aromatics along the reactor in liquid and solid phases.

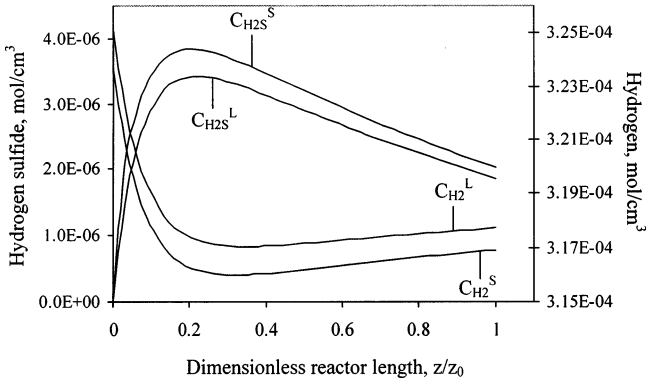

Figure 3. Concentrations of hydrogen and H_2S along the reactor in liquid and solid phases.

rate and mass transfer determines the overall shape of the hydrogen and H_2S profiles. The H_2S concentration rapidly increases and H_2 concentration decreases, which is due to the high reaction rate of the catalyst bed in the initial part of the reactor.

The HDS reaction is known to be inhibited by H_2S; hence, the inhibiting effect of H_2S will slow the reaction down to a point where mass transfer can keep up with it. This mass transfer in the different phases is very important in the modeling of HDT reactions, which is

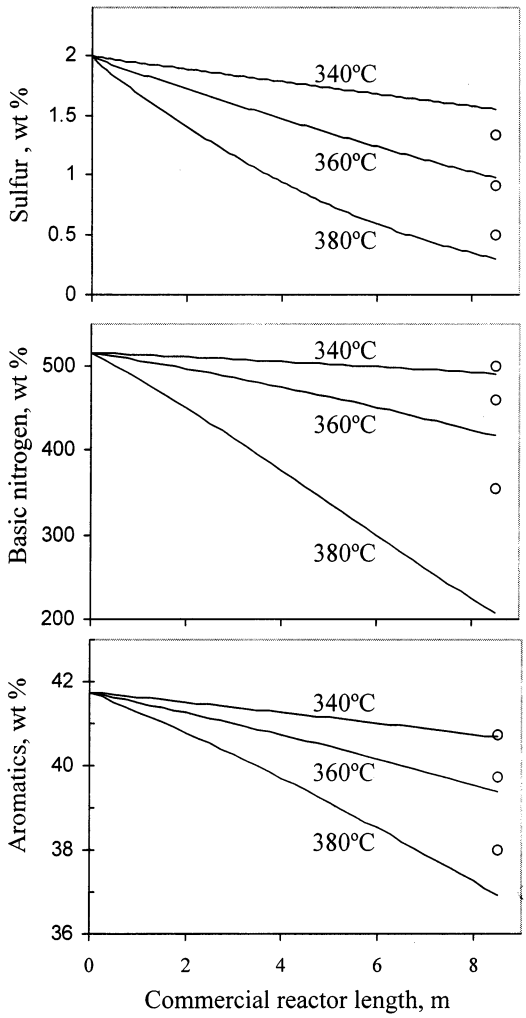

Figure 4. Concentrations of sulfur, basic nitrogen, and aromatics along the commercial reactor; symbols (○) represent experimental pilot-plant data, and the lines/curves represent the predicted values.

not taken into account in simpler models, i.e., the pseudo-homogeneous plug-flow model.

Modeling and Simulation of a Commercial HDT Reactor. After the model was verified to reproduce the experimental data obtained at pilot scale, it was applied to predict the expected behavior of a commercial HDT catalyst in an industrial unit. The commercial reactor information was taken from a design data book and from normal operation, and is as follows: internal diameter, 3 m; total length, 9.1 m; catalytic bed length, 8.5 m; and catalyst density, 816 kg/m^3. In this case, the energy balance given by eq 9 was solved simultaneously with mass-balance equations.

Commercial HDT units normally receive a high-purity hydrogen stream from reforming plants. To simulate the industrial unit, we used a stream with the following molar composition: 81.63% hydrogen, 3.06% H_2S, and 15.31% lights.

Figure 4 shows the predicted sulfur, basic nitrogen, and aromatics contents in the product, as a function of reaction temperature along the commercial reactor. The simulation was performed under the conditions of a pressure of 54 kg/cm^2, LHSV = 2 h^{-1}, and a H_2/oil ratio of 2000 ft^3/bbl to compare results with pilot-plant data. Predicted values from the isothermal pilot plant are also

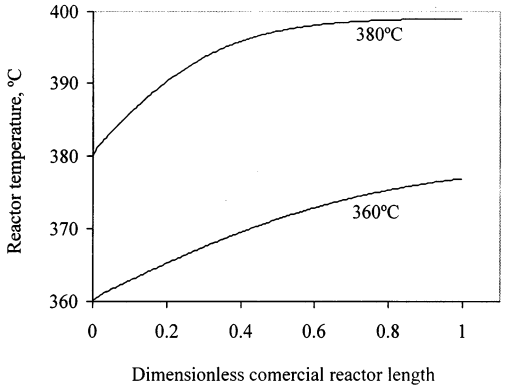

Figure 5. Predicted axial profiles of temperature in the commercial reactor.

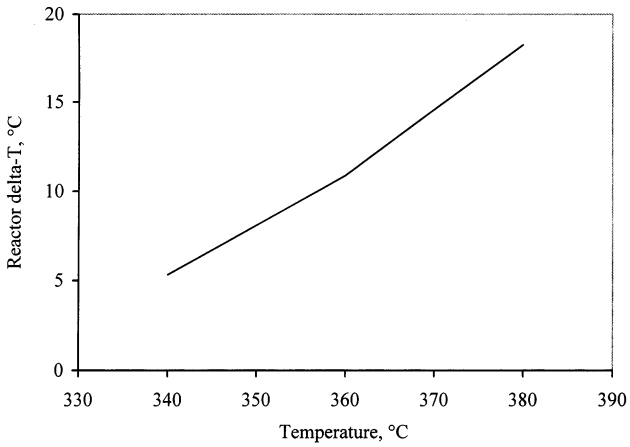

Figure 6. Temperature gradient (ΔT) of the commercial reactor unit.

included in this figure (denoted by the open circle symbol, "○"). Because a commercial reactor is operated at a higher average temperature, commercial operation generally is observed to give lesser contaminants contents than pilot-plant data. This behavior is quite clear at high temperatures.

Figure 5 shows the predicted axial profiles of reaction temperature in the commercial reactor. This figure shows that the increase in reaction temperature is higher in the initial part of the reactor, which is mainly due to the greater removal of contaminants that occurs in this zone.

The temperature gradient (ΔT) in the reactor is plotted against the inlet reactor temperature in Figure 6. As the reaction temperature is increased, the ΔT value also increases, which is due to the increment in reaction rate and, hence, in exothermic reaction. This increase in temperature also improves the removal of contaminants.

On the other hand, it is well-known that sulfur removal is strongly inhibited by the H_2S produced by the same HDS reaction at the sulfided sites of the bifunctional catalyst. This can be clearly seen in Figure 7, where simulations for both pilot and commercial reactors are shown. According to different authors, even low H_2S increments can reduce the HDS reaction rate by 5% and up to 50% with higher concentrations (10 mol %),[19,20] which is in good agreement with our pilot and commercial simulated results.

All these results indicate that, during catalyst screening in experimental reactors, which are commonly

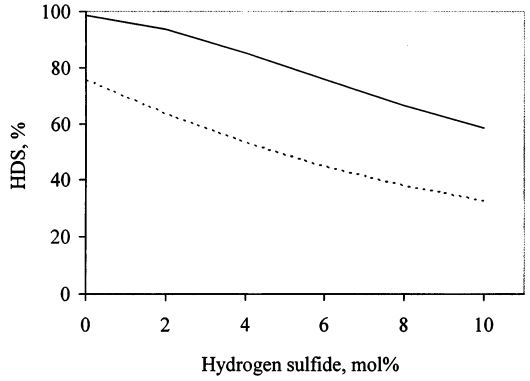

Figure 7. Effect of H_2S content on sulfur removal: (—) commercial reactor and (- - -) pilot reactor. Conditions were as follows: temperature, 380 °C; pressure, 54 kg/cm^2; LHSV = 2 h^{-1}; H_2/oil ratio, 2000 ft^3/bbl.

operated isothermally, the removal of contaminants, especially sulfur, is lower than the expected commercial behavior. Of course, this is dependent on the features of the experimental system. That is why pilot-plant experiments are normally compared with adiabatic operations by operating the pilot plant isothermally at a temperature that is equivalent to the average temperature of the commercial unit (i.e., the weighted average bed temperature (WABT), the average bed temperature (ABT), or the equivalent isothermal temperature (EIT)).[21] In our case, the objective was not the comparison of pilot-plant results with commercial data at equivalent conditions. We only tried to simulate the behavior of an industrial plant based on the kinetics and reactor modeling obtained from pilot-plant tests.

Another reason for the differences between pilot-plant and commercial results can be attributed to the incomplete catalyst contacting, which is a classical pilot-plant problem that can lead to underperformance. It is known that, during the operation of HDT trickle-bed reactors, the liquid hydrocarbon flows over the catalyst particles in films and rivulets from one particle to the next, and the vapor (mostly hydrogen) flows continuously through the remaining voids. These conditions cause poor catalyst utilization, because of incomplete catalyst wetting, axial dispersion, and restricted interphase mass transfer. Because commercial catalyst samples and real feedstocks are commonly used to conduct pilot-plant experiments (such as that in the present work), the ratio of the reactor small-scale length to catalyst particle diameter is very low, compared to that of commercial reactors, and low liquid velocities are used in small-scale reactors to match the LHSV values of commercial plants. These differences cause several problems in testing catalysts that have commercially applied sizes and shapes.

Finally, it is important to mention that we have taken kinetic information from different literature sources, and for better estimations of commercial HDT plant operation, it is necessary to design experiments to obtain kinetic data for a given catalyst and feed and to include these results in the reactor model balance equations.

(19) McCulloch, D. C. *Appl. Ind. Catal.* **1983**, *I*, 69.
(20) Gates, B. C.; Katzer, J. R.; Schuit, G. C. A. *Chemistry of Catalytic Processes*, 3th ed.; McGraw-Hill: New York, 1979.
(21) Yui, S.; Hubbard, P. *Oil Gas J.* **2000**, *98* (10), 57−60.

Conclusions

A reactor model reported in the literature for hydrodesulfurization (HDS) of oil fractions was extended to consider hydrogenation of aromatics (HDA) reactions and hydrodenitrogenation (HDN) reactions. The effect of reaction temperature was also included in the model.

Experimental data obtained in an isothermal pilot reactor, using commercial catalyst and feed under typical operating conditions, were used to determine the kinetic parameters of the reported models.

A commercial HDT reactor was simulated with the extended model developed in this work. The contaminant contents in the commercial reactor were observed to be less than the pilot-plant information. This behavior was attributed to the differences in average reactor temperature in both scales which were due to exothermic reactions.

Acknowledgment. The authors thank Instituto Mexicano del Petróleo for its financial support. M.A.R. also thanks CONACyT for financial support.

Nomenclature

a_L = Specific surface area, gas−liquid interface
a_S = Specific surface area, liquid−solid interface
C = Molar concentration
d_P = Particle diameter
k_f = Forward HDA rate constant
K_{H_2S} = Adsorption-equilibrium constant at infinite temperature
k^L = Gas−liquid mass-transfer coefficient
k_r = Reverse HDA rate constant
k^S = Liquid−solid mass-transfer coefficient
p = Partial pressure
R = Universal gas constant
r = Reaction rate
T = Temperature
u = Superficial velocity
z = Catalyst bed length

Subscripts

A = Aromatics
N_{NB} = Nonbasic nitrogen
N_B = Basic nitrogen

Superscripts

G = Gas
L = Liquid
S = Solid

Greek symbols

ϵ_L = Liquid-phase fraction
ϵ_G = Gas-phase fraction
ΔH_R = Heat of reaction (kJ/mol)
ρ_B = Catalyst bulk density

EF030172S